First analyses on a mechanical motion converter to produce electrical energy from sea wave

Domenico Curto
Department of Engineering
University of Palermo
Palermo, Italy
domenico.curto@deim.unipa.it

Vincenzo Franzitta
Department of Engineering
University of Palermo
Palermo, Italy

Andrea Guercio
Department of Engineering
University of Palermo
Palermo, Italy

Giovanni Napoli
Self employer
Palermo, Italy

***Abstract*—The exploitation of sea wave opens new horizon for suppling small islanded communities. With this goal the paper propones a prototypical device for the utilization of sea wave along the coastline. The device is based on a mechanical motion conversion, from an alternative rotation into unidirectional rotation in order to run commercial generators. First evaluations are here reported, demonstrating the feasibility of this solution.**

Keywords—sea wave, mechanical motion converter, WEC

I. Introduction

Renewable energies (RES) are universally considered as the future for the energy production, with the goal to limit the global warming and environmental pollutions [1]. However, the energy demand is characterized by an even increasing trend, mainly due to the Asian countries [2], as depicted in Fig. 1.

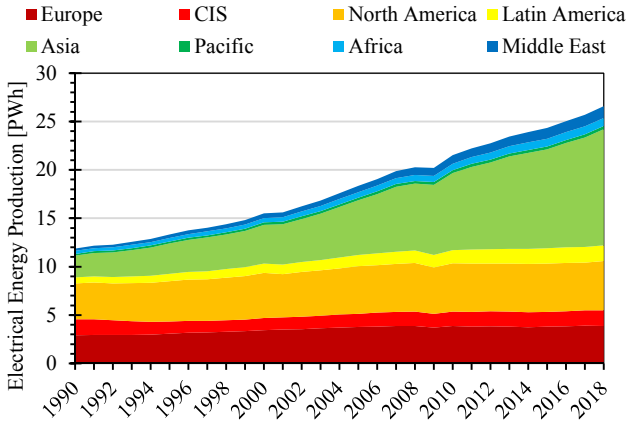

Fig. 1. Electrical energy production in the world

Indeed, the world electrical energy production has been expanding from 2.25 PWh/y in 1990 to 12.01 PWh/y in 2018, thus almost six times in about 30 years. Despite the installed power from RES is increasing very quickly (753.95 GW in 2000 to 2350.76 GW in 2018) [3], about two third of electrical energy is still annually produced from fossil fuels. Therefore, there are huge rooms for the introduction of more sustainable energy sources [4]–[6].

As well as environmental protection, the installation of RES offers the possibility to improve the energy independence of each country, avoiding the importation of fossil fuels from other territories [7].

As an example of the current energy mix adopted for the electricity production, the Italian power system is here reported.

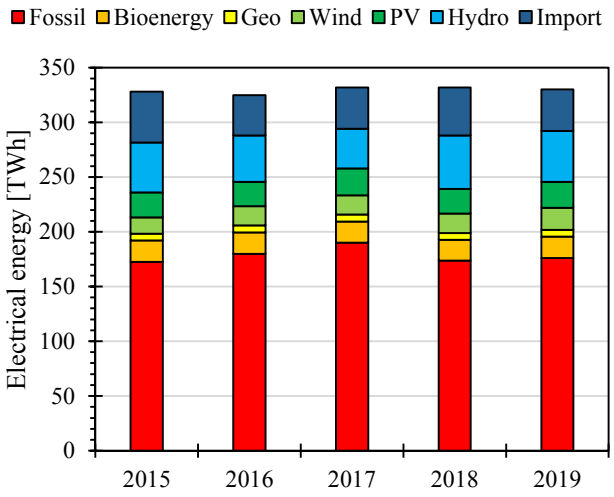

Fig. 2. Italian energy mix for the electrical production in the last five years.

In the last year, the share of electricity production from RES was equal to 39.67%, by using the following mix: fossil fuel (176.2 TWh), biofuels (19.6 TWh), geothermal energy (6.1 TWh), wind (20.2 TWh), solar (23.7 TWh) and hydropower (46.3 TWh). Furthermore, the energy demand was covered through the importation of 38.1 TWh from other countries [8].

The annual electrical energy demand was almost stable in the last years, as well as in many other developed countries. In any case, this example reveals the huge possibilities for the addiction of more RES in the energy mix [8], [9].

In this context, technologies like photovoltaic panels [10], wind turbines [11], hydro turbines and steam turbines supplied by geothermal energy [12] represent a valid solution, fully developed and commercially mature.

However, these RESs could not be implemented in some cases, such as in small islands, where the following peculiarities can be found [13]–[15]:

- High seasonal variation of the electrical demand, mainly due to the strong relevance of tourism.
- High operative costs for the electrical energy production, due to the small scales of plants and fuel importations.
- High maintenance costs because the power plants are significantly oversized in order to have enough backup power to face the seasonal variation of the energy demand and the potential failures of the diesel generators.
- Small standalone electrical grid with a limited innovation.
- Modest introduction of RES supplied plants because the environmental limitations to preserve the landscape.
- Strong dependence on fossil fuels, imported from other territories (mainland).

These peculiarities are quite common, for example, in all small islands in the Mediterranean Sea [16], [17]. For these reasons, new alternative renewable energy sources must be found and developed [18].

In this context, sea wave is considered a very promising energy source, especially in the context of small islands where the ratio between the energy demand and the availability of this source is very favorable [19], [20].

Furthermore, sea wave can exploit offshore and nearshore areas which are not used nowadays, avoiding the competition for the land use that could happen in case of other sources [21]–[23]. Indeed, wave supplied plants could be integrated in the existing harbors, performing the double function of protection of piers and energy production. At the same time supply chain and local job opportunities could be created [24].

A huge number of technologies have been assessed in the past, some of them also developed and tested in laboratories or open sea. Due to the multitude of solutions available in literature, different classifications are currently used, for example considering different aspects like the working principle, the orientation of device, the position in comparison to the sea level, the distance from the coastline, etc [25], [26]. The classification based on the direction of the wave propagation introduces the following definitions [27]–[29]:

- **attenuator**, a device parallelly oriented to the wave direction and adapting its shape to the wave profile.
- **point absorber**, a system characterized by an axial symmetry, in order to collect wave energy regardless of the wave direction [30], [31].
- **terminator**, a device that must be oriented perpendicularly to the wave direction on which the wave breaks to operate it.

Considering the working principle, the most popular definitions are:

- **Oscillating Water Column** (OWC), in which waves enter and exit a submarine chamber, in order to pressurize and the depressurize an air-filled chamber and run a wind turbine, specifically designed for this application.
- **Wave Body Activated** (WAB), a system that is composed by floating buoys, able to produce relative motion to run the energy converters.
- **Overtopping**, a device that firstly collects the kinetic energy of waves by filling a water reservoir and then produces electrical energy by spilling water from the reservoir and returning it to the sea through a low head hydro turbine.

There are a lot of examples in literature. Just some famous examples are: Kværner Brug [32], Limpet [33], Mighty Whale [34] for OWC systems; Wavebob [35], Powerbuoy [36], Pelamis [37], Archimede Wave Swing [38], Oyster [39] for WAB systems; finally, Tapchan [40], Wave Dragon [40] and Slotcone [41] for overtopping systems

Despite the huge number of proposed technologies, no commercial systems are available.

In this context, at the University of Palermo, Department of Engineering, an innovative device is under development. This technology is based on a mechanical motion converter able to transform an oscillating rotation into a unidirectional rotary motion and run commercial generators, like the same used for small wind turbines.

A prototype is firstly described in the following section. Some simulations are here reported, demonstrating the working principle of this technology.

II. Mechanical Motion Converter

The paper shows a mechanical motion converter that could be installed in the harbors for the exploitation of sea wave in order to produce electrical energy and at the same time protect the piers. The idea is illustrated in Fig. 3. A floating buoy is used to collect the mechanical energy of waves and produce a rotation around the main hinge of the device. The mechanical conversion is operated inside a gear box, that can be installed on the breakwaters. On the output axis, a commercial generator can be installed in order to produce electricity.

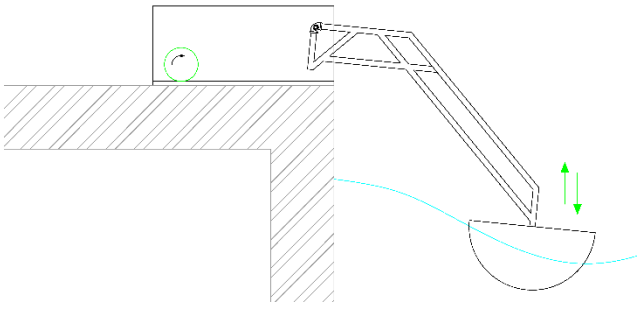

Fig. 3. The idea of the mechanical motion converter

The device is designed to exploit sea waves with a limited height. In particular, the prototype below described allows a total vertical oscillation until 1.06 m.

The conversion of bidirectional motion into unidirectional is entrusted to a system of freewheels, that are alternatively activated by the motion of the floating buoy.

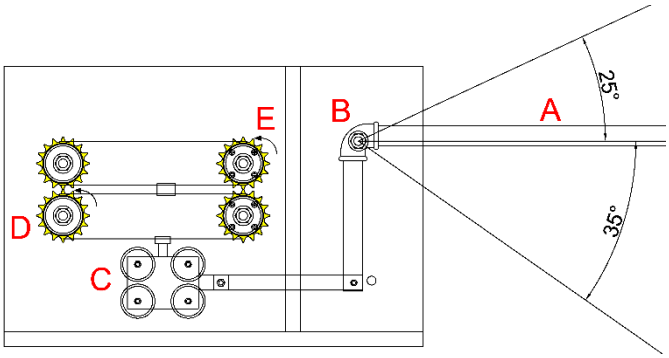

Fig. 4. Internal view of the prototype of mechanical motion converter

Indeed, as shown in Fig. 4, the rotation of the input bar A, around the hinge B, produces a translation of the slider C, causing the rotation of chains around the freewheels D and E.

These ones are mounted in order to transfer torque in different times: freewheel D is active if the slider is moved from the left to the right side; on the contrary, freewheel E is activated.

In this way, two impulsive unidirectional rotations are available in the corresponding axes D and E. Both motions are externally transferred to a single axis from the blue wheels by using chains. As shown in Fig. 5 and Fig. 6, other axes equipped with different wheels are introduced to increase the angular speed and achieve the optimal range for the generator.

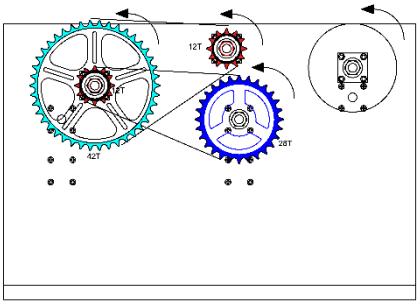

Fig. 5. External left side view of the prototype

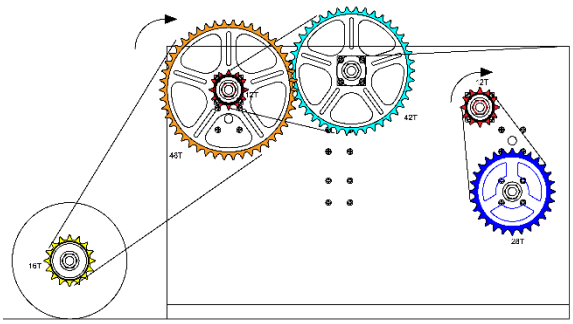

Fig. 6. External right side view of the prototype

A freewheel is introduced in axis before the alternator, where a flywheel is installed to smooth the angular speed applied to the generator and consequently regularize the electricity production.

In comparison with other technologies, there are several advantages:

- Absence of pressurized fluid
- A limited number of components
- The use of commercial components, minimizing the costs for designing and development.

A picture of the prototype is reported in Fig. 7. A 24V DC generator is installed at the output axis and connected to a rheostat.

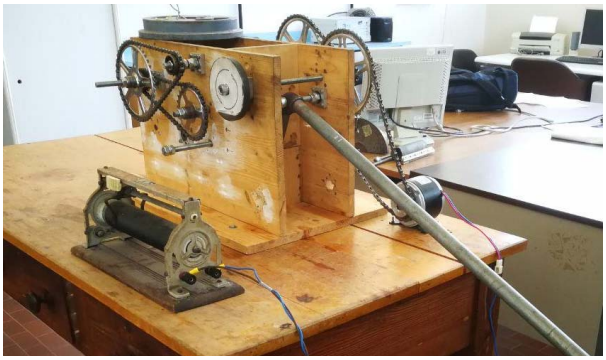

Fig. 7. View of the prototype

III. Correlation between the input and output rotations

Analyzing the kinematic reported in Fig. 4, the angular rotation of the output axis can be evaluated in the following way.

The system is designed with the properties that if the input bar is horizontal the same is the crank connecting the slider. Assuming as absolute reference of x axis the center of the hinge and considering positive the clockwise rotation of the input bar, Eq. 1 can be derived to describe the position of the slider pin.

$$x(\vartheta_{in}) = -\sqrt{b^2 - l^2(1 - cos\,\vartheta_{in})^2} + l\,sin\,\vartheta_{in} \qquad (1)$$

In this equation, b is the length of the crank and l the shorter length of the input bar (178 mm and 190 mm respectively).

It can be observed that the differentiation of Eq. 1 is:

$$\frac{dx}{d\vartheta_{in}} = \frac{l^2\,sin\,\vartheta_{in}\,(1 - cos\,\vartheta_{in})}{\sqrt{b^2 - l^2(1 - cos\,\vartheta_{in})^2}} + l\,cos\,\vartheta_{in} \qquad (2)$$

If ϑ_{in} is equal to zero, Eq. 2 becomes equal to l. Considering the lengths b and l, and the operative limitations of the maximal stroke available in the device, Eq. 2 can be still approximated equal to l, with an average error equal to 4.18% (the maximum is for $\vartheta = 25°$, in which the error achieves the value of 13.62%).

Thus, Eq. 1 can approximated to Eq. 3 in case of small rotation:

$$x(\vartheta_{in}) \approx l\vartheta_{in} \qquad (3)$$

Consequently, the external angular rotation, of the first freewheel is equal to:

$$\vartheta_1 \approx \vartheta_{in} \frac{l}{r_1} \tag{4}$$

where r_1 is the external radius of the freewheel. In the following axis, the rotation becomes unidirectional thanks to the sum of two unidirectional rotations from the freewheels D and E. Thus, the rotation of this axis is equal to:

$$\vartheta_2 = |\vartheta_1| k_{2,1} \approx |\vartheta_{in}| \frac{l}{r_1} k_{2,1} \tag{5}$$

The term $k_{2,1}$ represents the transmission factor between axes 2 and 1.

As introduced above, the other wheels are used to increase the angular speed. Therefore, the angular rotation in the output axis, is equal to:

$$\vartheta_4 \approx |\vartheta_{in}| \frac{l}{r_1} k_{2,1} k_{3,2} k_{4,3} \tag{6}$$

However, in term of angular speed should be noted that the output axis is designed to store kinetic energy into the flywheel thus, Eq. 7 is introduced.

$$\begin{cases} if\ \omega_3 k_{4,3} < \omega_4 \rightarrow \left(I_{fw} + I_a \frac{1}{k_a^2}\right) \frac{d\omega_4}{dt} = -\tau_e - \tau_f \\ else \rightarrow \omega_4(t) = \omega_3 k_{4,3}(t) = \gamma_0 |\omega_{in}(t)| \end{cases} \tag{7}$$

According the sized of prototype, γ_0 is equal to 491.

In fact, thanks to the freewheel, the output axis rotates at the angular speed set by the mechanical converter. Vice versa, if the angular speed produced by the rotation of the input bar is lower than the instantaneous angular speed of output axis, the output wheel does not receive torque from the previous axis, and consequently reduces its regime removing kinetic energy from the flywheel.

IV. Simulation

The mechanical motion converter was simulated considering the application of a testing mass on the input bar and producing a descending motion of the weight.

During this transient, the 2nd Newton law was applied to the hinge of the input bar. The main terms are:

- The torque $\tau_g\langle\vartheta\rangle$ due to the testing mass M and the distributed mass m of the input bar, having a length *L*
- The friction torque $\tau_f\langle\frac{d\vartheta}{dt}\rangle$ manly due to the generator
- The torque reaction $\tau_e\langle\frac{d\vartheta}{dt},\vartheta\rangle$ due to the electricity production
- The inertia $I\langle\vartheta\rangle$ due to the testing mass, the distributed mass of the input bar, and the inertia of flywheel I_{fw} and generator I_e, reported to the hinge.

Thus, the governor equation is obtained. Eq. 8 presents many nonlinear parameters, depending on the instantaneous angular position of the input bar. About the generator, a linear trend was assumed as relation between the open circuit voltage and its angular speed. The term R_L is the electrical load resistance, R_g the internal resistance of generator. V_{ref} is the rated voltage (24 V) at the rated speed of the machine ω_{ref} (2550 rpm) according to the plate data of the machine. Finally, the term $sgn\left(\frac{d\vartheta}{dt}\right)$ represents the signum function of angular speed.

$$\begin{gathered} \tau_g\langle\vartheta\rangle - \tau_f\langle\frac{d\vartheta}{dt}\rangle\gamma\langle\vartheta\rangle - \tau_e\langle\frac{d\vartheta}{dt},\vartheta\rangle\gamma\langle\vartheta\rangle = I\langle\vartheta\rangle\frac{d^2\vartheta}{dt^2} \\ \tau_f\langle\frac{d\vartheta}{dt}\rangle = \tau_f\, sgn\left(\frac{d\vartheta}{dt}\right) \\ \tau_g\langle\vartheta\rangle = -\left(ML + \frac{mL^2}{2}\right) g\cos\vartheta \\ \tau_e\langle\frac{d\vartheta}{dt},\vartheta\rangle\gamma\langle\vartheta\rangle = \frac{1}{R_L + R_g}\left(\frac{V_{ref}}{\omega_{ref}}\right)^2 \gamma^2\langle\vartheta\rangle\left|\frac{d\vartheta}{dt}\right| sgn\left(\frac{d\vartheta}{dt}\right) \\ I\langle\vartheta\rangle = ML^2 + \frac{mL^3}{3} + \left(\frac{I_{fw}}{k_a^2} + I_e\right)\gamma^2\langle\vartheta\rangle \end{gathered} \tag{8}$$

Since this simulation considered the entire stroke of the pulley, the approximation in Eq. 3 cannot be adopted. Eq. 9 was used instead.

$$\gamma\langle\vartheta\rangle = \left[\frac{l\sin\vartheta_{in}\,(1-\cos\vartheta_{in})}{\sqrt{b^2 - l^2(1-\cos\vartheta_{in})^2}} + \cos\vartheta_{in}\right]\gamma_0 \tag{9}$$

When the input bar ends its motion, the electrical generator continues to rotate, thanks to the kinetic energy stored by the generator itself and the flywheel. To describe this transient, the generator axis is considered introducing the subscription "e" in Eq. 10.

$$\begin{gathered} -\left[\tau_f + \tau_{e,e}\langle\frac{d\vartheta_e}{dt}\rangle\right] sgn\left(\frac{d\vartheta}{dt}\right) = \left(\frac{I_{fw}}{k_a^2} + I_e\right)\frac{d^2\vartheta_e}{dt^2} \\ \tau_{e,e}\langle\frac{d\vartheta_e}{dt},\vartheta\rangle = \frac{1}{R_L + R_g}\left(\frac{V_{ref}}{\omega_{ref}}\right)^2\left|\frac{d\vartheta_e}{dt}\right| \end{gathered} \tag{10}$$

The same model can be adopted if the weight is applied through a pulley (having a negligible inertia), in order to produce an ascending motion of the bar. The only change is represented by the signum before the testing mass M in the third Eq. 8.

The testing mass was varied, assuming alternatively the values 10 kg, 20 kg, 30 kg. The load resistance was regulated to the values 5 Ω, 10 Ω and 20 Ω.

About the friction torque τ_f (measured on the generator) a value of 0.0886 Nm was measured at the laboratory. The internal resistance is equal to 0.25 Ω.

The energy analysis of all simulation is reported in Table I and Table II, respectively for the downward motion and upward motion of the input bar.

TABLE I. Energy distribution in downward simulations

Mass [kg]	R load [Ω]	Energy input [J]	Energy to load [J]	Loss by Joule [J]	Residual kinetic [J]	Loss by friction [J]
10	5	116.40	62.88	3.14	0.28	50.10
10	10	116.40	49.29	1.23	0.42	65.46
10	20	116.40	33.80	0.42	0.52	81.66
20	5	220.18	143.98	7.20	1.61	67.39
20	10	220.18	116.63	2.92	2.11	98.52
20	20	220.18	83.77	1.05	2.42	132.94
30	5	323.96	226.94	11.35	4.14	81.54
30	10	323.96	188.04	4.70	5.13	126.09
30	20	323.96	139.22	1.74	5.72	177.28

TABLE II. ENERGY DISTRIBUTION IN UPWARD SIMULATIONS

Mass [kg]	R load [Ω]	Energy input [J]	Energy to load [J]	Loss by Joule [J]	Residual kinetic [J]	Loss by friction [J]
10	5	91.17	30.48	1.52	0.13	59.03
10	10	91.17	25.35	0.63	0.24	64.95
10	20	91.17	17.69	0.22	0.33	72.93
20	5	194.95	91.38	4.57	1.23	97.77
20	10	194.95	76.32	1.91	1.72	115.00
20	20	194.95	55.21	0.69	2.04	137.01
30	5	298.73	155.87	7.79	3.50	131.57
30	10	298.73	132.39	3.31	4.53	158.51
30	20	298.73	98.40	3.31	5.14	193.97

The corresponding electrical efficiency is reported in Fig. 8. It is possible to observe that the downward motion has an average efficiency higher than the corresponding upward condition. The increment of the load resistance reduces the electrical efficiency. This is due by the fact that the alternator runs for more revolutions, thus the loss by friction are incremented. At the same time, a marginal increment of the residual kinetic energy of the testing mass is observed. On the contrary, the internal loss by Joule effect inside the generator are reduced.

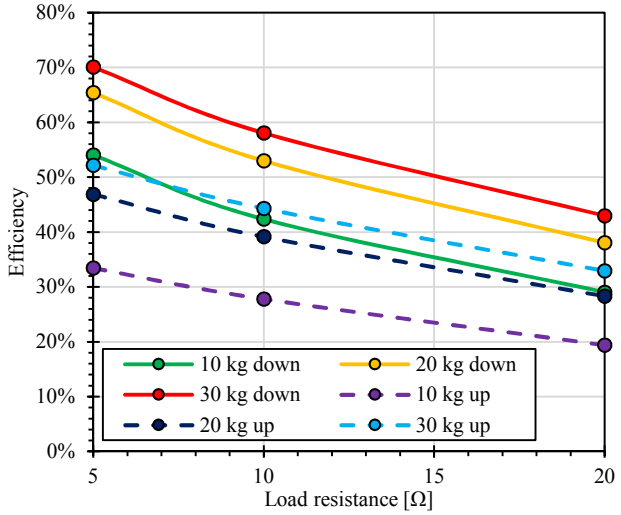

Fig. 8. Comparison of the electrical efficiency in all simulations.

As an example, the rotation of the input bar and the generator are reported in Fig. 9, considering the case with the highest efficiency for downward and upward motions (30 kg and 5 Ω). In this graph, it is possible to identify the instant when the transmission between the generator and the input bar is disconnected by the freewheels. Indeed, from this moment on, the generator continues to rotate thanks to its inertia and the inertia of the flywheel.

The corresponding voltage and power trends are reported in Fig. 10. It is possible to observe an increasing trend for both parameters when the weight can transfer torque to the generator. After the disconnection, both trends decrease.

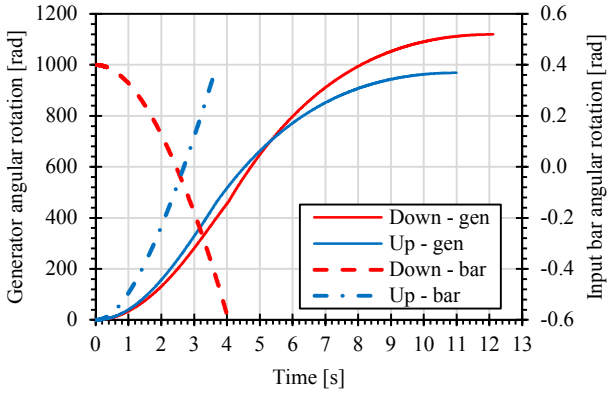

Fig. 9. Comparison of the angular rotation of the input bar and the generator in case downward and upward motion, with a testing weight of 30 kg and a load resistance of 5 Ω.

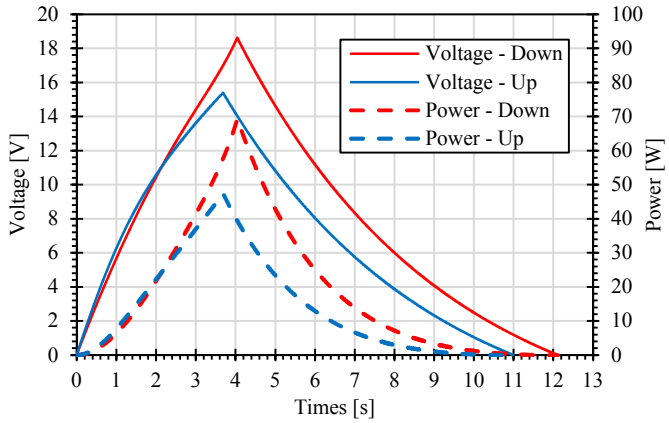

Fig. 10. Voltage and power trends on the electrical load, with a testing weight of 30 kg and a load resistance of 5 Ω.

V. CONCLUSION

An innovative motion converter was presented, with the target of sea wave exploitation close the coastline. A small prototype was realized to demonstrate the working principle. Preliminary simulations were performed in order to evaluate the energy performance with different electrical loads and weights applied to the input bar (simulating the reaction of a floating buoy).

The benefits of this kind of systems are related to the possibility to use commercial components, minimizing the costs for the development.

There are rooms for an improvement of the entire system, for example, modifying the relative position of the components, the length of the input bar, as well as the reduction of the internal loss by friction for example improving the lubrification of bearings. However, according to the simulation, interesting energy efficiency can be achievement, up to 70% as reported in Fig. 8.

Next step will concern experiments in a laboratory, in order to confirm the simulation, then first experiments could be performed in the tank, in order to evaluate the hydrodynamic

interactions between the buoy and the mechanical motion converter.

ACKNOWLEDGMENT

The authors wish to thank Giovanni Napoli for allowing the analysis of its prototype, subject of patent n. PA2014A000005. This work is realized thanks to the technical support of Engosys Enterprise.

REFERENCES

[1] M. Bissiri, P. Moura, N. C. Figueiredo, and P. P. Silva, "Towards a renewables-based future for West African States: A review of power systems planning approaches," *Renew. Sustain. Energy Rev.*, vol. 134, no. April, p. 110019, 2020.

[2] H. Chen, Z. Wang, S. Xu, Y. Zhao, Q. Cheng, and B. Zhang, "Energy demand, emission reduction and health co-benefits evaluated in transitional China in a 2 °C warming world," *J. Clean. Prod.*, vol. 264, p. 121773, 2020.

[3] IRENA, "Renewable Power Generation Costs in 2017," 2018.

[4] F. G. Kiburi, C. L. Kanali, G. M. Kituu, P. O. Ajwang, and E. K. Ronoh, "Performance evaluation and economic feasibility of a solar-biomass hybrid greenhouse dryer for drying Banana slices," *Renew. Energy Focus*, vol. 34, no. 00, pp. 60–68, 2020.

[5] S. Fuentes, R. Villafafila-Robles, P. Olivella-Rosell, J. Rull-Duran, and S. Galceran-Arellano, "Transition to a greener Power Sector: Four different scopes on energy security," *Renew. Energy Focus*, vol. 33, no. June, pp. 23–36, 2020.

[6] V. Franzitta, A. Viola, M. Trapanese, and D. Milone, "A Procedure to Evaluate the Indoor Global Quality by a Sub Objective-Objective Procedure," *Adv. Mater. Res.*, vol. 734–737, no. August, pp. 3065–3070, Aug. 2013.

[7] T. C. Moralesa, V. R. Olivab, and L. F. Velázquezc, "Hydrogen from renewable energy in Cuba," *Energy Procedia*, vol. 57, pp. 867–876, 2014.

[8] Terna S.p.A., "Publicazioni Statistiche." [Online]. Available: https://www.terna.it/it/sistema-elettrico/statistiche/pubblicazioni-statistiche. [Accessed: 11-Aug-2020].

[9] V. Franzitta and G. Rizzo, "Renewable energy sources: A Mediterranean perspective," in *2010 2nd International Conference on Chemical, Biological and Environmental Engineering*, 2010, no. Icbee, pp. 48–51.

[10] V. Muteri *et al.*, "Review on Life Cycle Assessment of Solar Photovoltaic Panels," *Energies*, vol. 13, no. 1, p. 252, Jan. 2020.

[11] J. G. Njiri and D. Söffker, "State-of-the-art in wind turbine control: Trends and challenges," *Renew. Sustain. Energy Rev.*, vol. 60, pp. 377–393, 2016.

[12] I. Lee, J. W. Tester, and F. You, "Systems analysis, design, and optimization of geothermal energy systems for power production and polygeneration: State-of-the-art and future challenges," *Renew. Sustain. Energy Rev.*, vol. 109, no. January, pp. 551–577, 2019.

[13] E. K. Stuart, "Energizing the island community: A review of policy standpoints for energy in small island states and territories," *Sustain. Dev.*, vol. 14, no. 2, pp. 139–147, Apr. 2006.

[14] IRENA, "Transforming small-island power systems: Technical planning studies for the integration of variable renewables," Abu Dhabi.

[15] V. Franzitta, D. Curto, D. Milone, and M. Trapanese, "Energy Saving in Public Transport Using Renewable Energy," *Sustainability*, vol. 9, no. 1, p. 106, Jan. 2017.

[16] I. Kougias, S. Szabó, A. Nikitas, and N. Theodossiou, "Sustainable energy modelling of non-interconnected Mediterranean islands," *Renew. Energy*, vol. 133, pp. 930–940, Apr. 2019.

[17] J. P. Sierra, C. Mösso, and D. González-Marco, "Wave energy resource assessment in Menorca (Spain)," *Renew. Energy*, vol. 71, pp. 51–60, 2014.

[18] G. Ciulla, V. Franzitta, V. Lo Brano, A. Viola, and M. Trapanese, "Mini Wind Plant to Power Telecommunication Systems: A Case Study in Sicily," *Adv. Mater. Res.*, vol. 622–623, no. June 2017, pp. 1078–1083, Dec. 2012.

[19] D. Curto, S. Favuzza, V. Franzitta, R. Musca, M. A. Navarro Navia, and G. Zizzo, "Evaluation of the optimal renewable electricity mix for Lampedusa island: The adoption of a technical and economical methodology," *J. Clean. Prod.*, vol. 263, p. 121404, Aug. 2020.

[20] G. Emmanouil, G. Galanis, C. Kalogeri, G. Zodiatis, and G. Kallos, "10-year high resolution study of wind, sea waves and wave energy assessment in the Greek offshore areas," *Renew. Energy*, vol. 90, pp. 399–419, 2016.

[21] L. Späth, "Large-scale photovoltaics? Yes please, but not like this! Insights on different perspectives underlying the trade-off between land use and renewable electricity development," *Energy Policy*, vol. 122, no. March, pp. 429–437, 2018.

[22] I. Capellán-Pérez, C. de Castro, and I. Arto, "Assessing vulnerabilities and limits in the transition to renewable energies: Land requirements under 100% solar energy scenarios," *Renew. Sustain. Energy Rev.*, vol. 77, no. May, pp. 760–782, 2017.

[23] D. Curto, S. Neugebauer, A. Viola, M. Traverso, V. Franzitta, and M. Trapanese, "First Life Cycle Impact Considerations of Two Wave Energy Converters," in *2018 OCEANS - MTS/IEEE Kobe Techno-Oceans (OTO)*, 2018, pp. 1–5.

[24] D. Curto, A. Viola, V. Franzitta, M. Trapanese, and F. Cardona, "A New Solution for Sea Wave Energy Harvesting, the Proposal of an Ironless Linear Generator," *J. Mar. Sci. Eng.*, vol. 8, no. 2, p. 93, Feb. 2020.

[25] T. Aderinto and H. Li, "Ocean Wave energy converters: Status and challenges," *Energies*, vol. 11, no. 5, pp. 1–26, 2018.

[26] A. Pecher and J. P. Kofoed, *Handbook of Ocean Wave Energy*, vol. 7. Cham: Springer International Publishing, 2017.

[27] B. Drew, A. R. Plummer, and M. N. Sahinkaya, "A review of wave energy converter technology," *Proc. Inst. Mech. Eng. Part A J. Power Energy*, vol. 223, no. 8, pp. 887–902, Dec. 2009.

[28] V. Franzitta, D. Curto, D. Rao, and A. Viola, "Hydrogen Production from Sea Wave for Alternative Energy Vehicles for Public Transport in Trapani (Italy)," *Energies*, vol. 9, no. 10, p. 850, Oct. 2016.

[29] V. Franzitta, A. Viola, and M. Trapanese, "Design of a transverse flux machine for power generation from seawaves," *J. Appl. Phys.*, vol. 115, no. 17, p. 17E712, May 2014.

[30] V. Piscopo, G. Benassai, R. Della Morte, and A. Scamardella, "Cost-based design and selection of point absorber devices for the Mediterranean Sea," *Energies*, vol. 11, no. 4, pp. 1–23, 2018.

[31] V. Di Dio, V. Franzitta, D. Milone, S. Pitruzzella, M. Trapanese, and A. Viola, "Design of Bilateral Switched Reluctance Linear Generator to Convert Wave Energy: Case Study in Sicily," *Adv. Mater. Res.*, vol. 860–863, pp. 1694–1698, Dec. 2013.

[32] R. Bhattacharyya and M. E. McCormick, "Wave Power Activities in Northern Europe," in *Wave Energy Conversion*, 1st ed., Elsevier Science, 2003, pp. 95–123.

[33] A. F. O. Falcão and J. C. C. Henriques, "Oscillating-water-column wave energy converters and air turbines: A review," *Renew. Energy*, vol. 85, no. January, pp. 1391–1424, 2016.

[34] DTI, "Near Shore Floating Oscillating Wave Column: Prototype Development and Evaluation," 2004.

[35] K. Tarrant and C. Meskell, "Investigation on parametrically excited motions of point absorbers in regular waves," *Ocean Eng.*, vol. 111, pp. 67–81, 2016.

[36] S. Patel, "Ocean Power Technologies Deploys Commercial PowerBuoy with Energy Storage," 2016. [Online]. Available: https://www.powermag.com/ocean-power-technologies-deploys-commercial-powerbuoy-energy-storage/. [Accessed: 09-Aug-2019].

[37] Y. Hong, R. Waters, C. Boström, M. Eriksson, J. Engström, and M. Leijon, "Review on electrical control strategies for wave energy converting systems," *Renew. Sustain. Energy Rev.*, vol. 31, pp. 329–342, Mar. 2014.

[38] J. Blackledge, E. Coyle, D. Kearney, R. McGuirk, and B. Norton, "Estimation of wave energy from wind velocity," *Eng. Lett.*, vol. 21, no. 4, pp. 158–170, 2013.

[39] P. Evans, "Oyster ocean power system to provide 1 GW by 2020," *New Atlas*, 2009. [Online]. Available: https://newatlas.com/oyster-ocean-power-system/11180/.

[40] A. F. de O. Falcão, "Wave energy utilization: A review of the technologies," *Renew. Sustain. Energy Rev.*, vol. 14, no. 3, pp. 899–918, Apr. 2010.

[41] M. Buccino, D. Banfi, D. Vicinanza, M. Calabrese, G. Del Giudice, and A. Carravetta, "Non breaking wave forces at the front face of Seawave Slotcone Generators," *Energies*, vol. 5, no. 11, pp. 4779–4803, 2012.